215718-9

ABCM

THEORETICAL AND EXPERIMENTAL ANALYSIS FOR THE RETARDING TORQUES OF A TURBINE FLOW METER

Ferreira, V.C.S. and Favaretto C.F.
Department of Mechanical Engineering
Federal University of Rio Grande do Sul
90050-170, Porto Alegre, RS, Brazil

SUMMARY

Many theoretical and experimental studies have been made to access the actual values of the retarding torques of a turbine flowmeter but because of the complex flow interaction and their tiny value this has been an uneasy task. The aim of this work is to obtain a consistent analytical expression, experimentally established, which represents the equilibrium equation of a turbine meter for the whole flow range.

INTRODUCTION

Turbine type flow meter is an especial turbomachine with no power output. When running at constant speed, in equilibrium, the driving torque is equal to the retarding ones. The retarding torques are due to the blade surface (T_s) and rotor hub skin friction (T_h), due to the bearing friction (T_{brl}), due to the friction between the disk surface of the hub and the support (T_f), due to the drag at blade tip clearance (T_{bt}), and due to the retarding force caused by the pickup (T_p), when a magnetic type is used. The T_d, which provides the turbine motion, comes from the mean flow energy through the rotor blades. This torque may be calculated using the angular momentum analysis or the airfoil theory applied for a turbomachinery, as used by Blows (1981), Rubin et. al. (1965) and Thompson and Grey (1970). Eq. (1) below, presents the equilibrium equation in this situation. Fig. 1, from Favaretto (1995), illustrates all the involving torques in a running turbine meter.

$$T_d = \Sigma T_R = T_s + T_h + T_f + T_{bt} + T_{brl} + T_p \qquad (1)$$

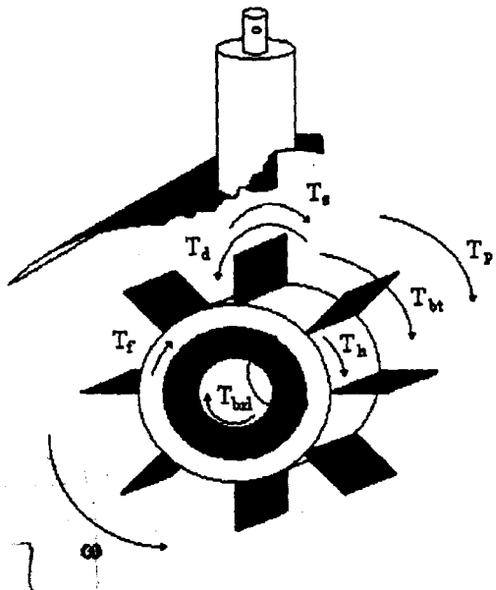

Figure 1 - Driving and retarding torques

Many theoretical approaches and experimental studies have been made to access the actual values of the retarding torques but, because of the complex flow interaction with the meter and their tiny values, performing each torque has been a difficult task. The aim of the present work is to obtain a consistent analytical expression, experimentally established, which represents the equilibrium equation of a turbine flow meter for the whole flow range. The purpose of this study is also to better understand the flow behaviour in order to design new prototypes and/or improve the performance of the old ones.

In the present paper, two retarding torques measured experimentally are presented. The other ones were analytically performed by using expressions which came from the technical literature or especially here developed. The equilibrium equation for the whole flow range of the prototype tested is also presented and discussed.

The bearing retarding force and the magnetic pickup drag were measured experimentally using a special developed test rig. The effect of the magnetic pickup on the calibration curve is also analysed. An optical pickup, with no drag effect, was developed. A comparison between the two situations with and without the magnetic force is analysed through the calibration curve of the turbine meter tested.

EXPERIMENTAL ANALYSIS

Bearing Retarding Torque. The test rig used for measuring the bearing retarding force was described by Favaretto (1995) and comprises a driving motor with a continuous speed control, a load cell using strain gages, a dynamic amplifier bridge and a computer data acquisition system. A single ball bearing and a complete turbine rotor with double bearings were tested for several rotational speed within the flow range of the turbine meter, according to its calibration curve. The tests were taken with three different fluids: air, water and low viscosity oil. Fig. 2 illustrates the test rig developed.

Measuring the bearing retarding force consisted of recording the strain signal from the load cell pressed by a punctual contact of the blade surface of the turbine meter rotor. The internal ring of the ball bearing rotates driven by the servo-motor at a selected speed. The rotational velocity ranged from 200 RPM up to 3000 RPM, which is within the flow range of the prototype tested. Fig. 3 shows a particular test with oil as the working fluid and at the rotational speed of 1550 RPM. The turbine rotor

ESCOLA DE ENGENHARIA

was tested in the same rig, showed in Fig. 2, replacing the ball bearing.

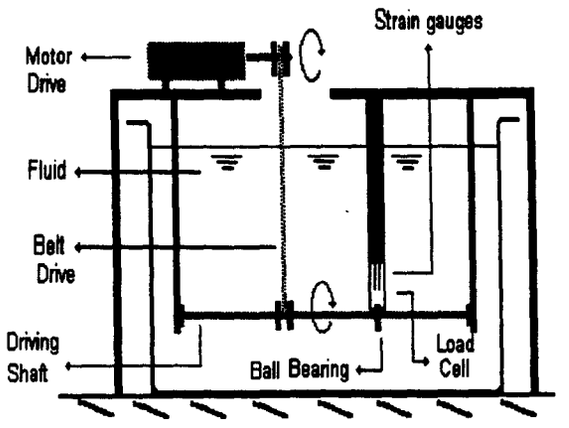

Figure 2 - Test rig for measuring the bearing drag torque

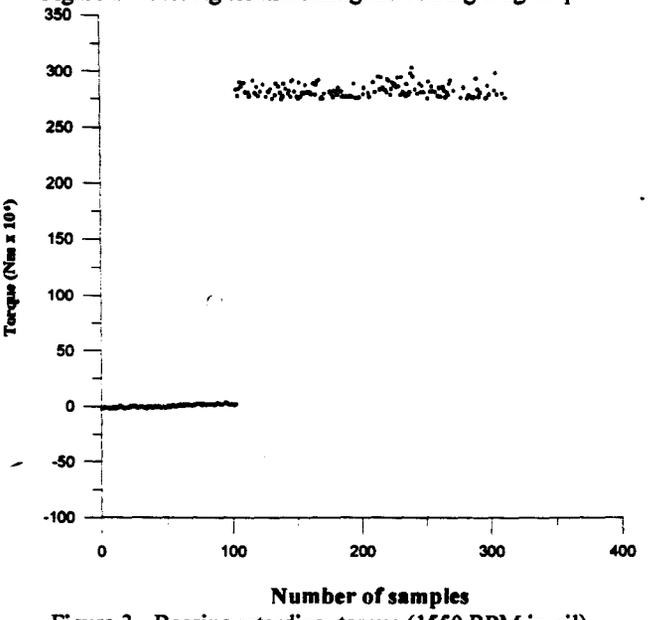

Figure 3 - Bearing retarding torque (1550 RPM in oil)

The data acquisition system is able to record samples for the computer hard disk at a frequency of 2.6 Khz. Each test consisted of an average of 500 sample points with the first 100 samples acquired without load and the remaining 400 under stress. The plot discontinuity shown in figure 3 represents, practically, this situation.

The load cell was particularly developed for very small forces. It consists of a rectangular stainless steel blade with a thickness of 0.2 mm and fixed onto a stiff support. The load cell is able to record forces as low as 0.002 N. A complete analysis for a particular case is formed for several tests in different rotational speed.

The experimental results are presented in Figs. 4, 5 and 6. Fig. 4 shows the relationship between the bearing drag retarding torque for a single glass ball bearing in air and in water medium. Fig. 5 presents for the same ball bearing retarding torque now operating in a low viscosity oil (31.2 Cst at 40°C). The last figure, Fig. 6, shows the results for a complete turbine meter rotor in water. The rotor hub comprises two glass ball bearings, similar to the previously tested one, in parallel arrangement and running inside the water. From figure 6 one can see the linear characteristic of the relationship between the bearing retarding torque and the rotational speed N (RPM) of the rotor:

$$T_{brl} = 4.19956 \times 10^{-6} N \quad (2)$$

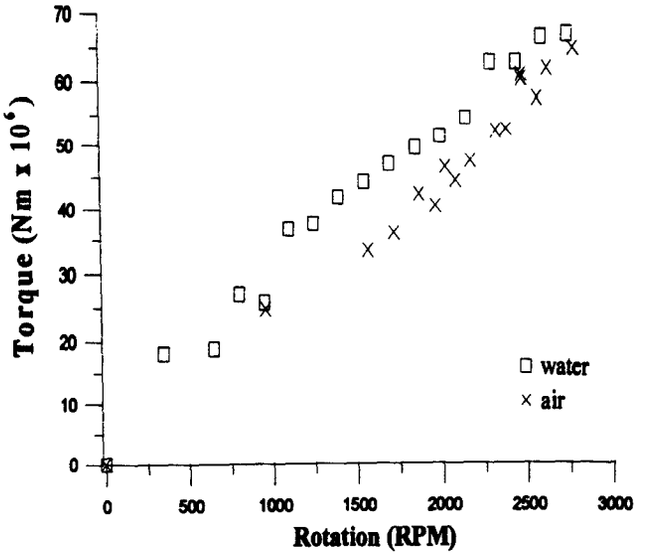

Figure 4 - Bearing torque x Rotational speed

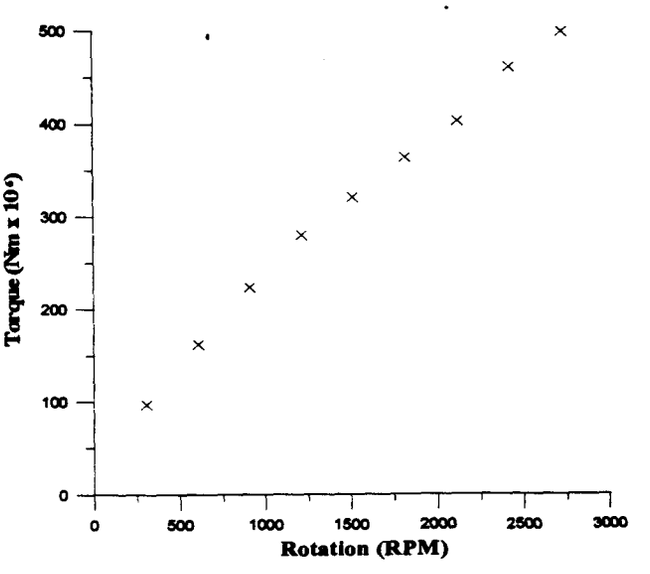

Figure 5 - Bearing torque x Rotational speed (Fluid Oil)

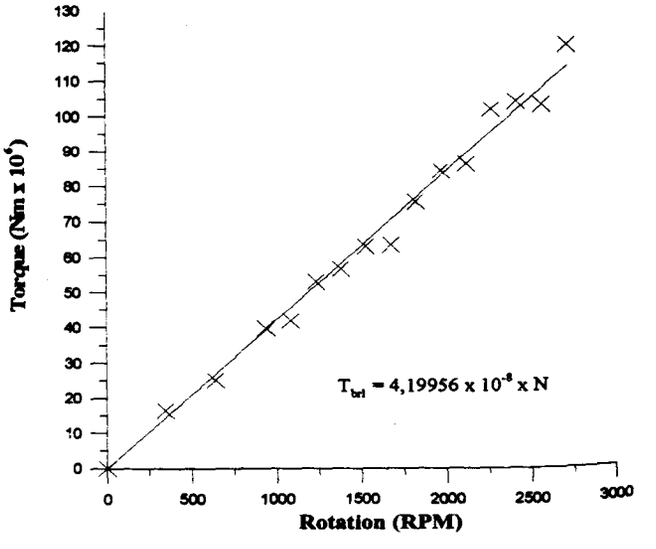

Figure 6 - Bearing Torque x Rotational Speed
(Turbine rotor prototype in water)

The experimental results showed a linear behaviour with small of uncertainty. The uncertainty ranged from ± 3% up to ± 8.5% with the small values for the oil tests, the medium values

for water and the high values for the air tests. One important effect noticed during the measuring tests was the vibration induced by the load cell, itself. Tiny transient effects produced in the torque transmission from the motor, pulley, and/or from the belt drive were transmitted up to the turbine rotor and amplified by the *load cell blade*. This fact produced a torque fluctuation dependent on the fluid used. In oil, due to the dumping effect caused by the high viscosity, small fluctuations were noticed, whereas in air, the opposite was found. Measurements close to the natural frequency of the load cell blade were also avoided due to the resonance effects which caused high torque fluctuation.

It is important to compare the magnitude of the retarding torque measured in different media. As it was expected, the torque measured in oil assumed higher values than in water. This was probably, because the oil viscosity (absolute, μ or kinematics viscosity, ν) is bigger than the water viscosity. The same comparison between water and air is not so clear. It is interesting to notice that the retarding torque measured for both fluids are of the same order of magnitude being the absolute viscosity of the water about fifty times the air viscosity and the kinematic viscosity of the air eighteen times the water.

Magnetic Pickup Retarding Torque. The magnetic retarding effect was measured using the same previous rig, though, in a slight different arrangement. Instead of spinning the internal ring of the ball bearing, as for the bearing drag tests, the servo-motor moves the load cell upwards pressing the punctual contact of the blade rotor. Fig. 7 characterises the physical arrangement of the test rig.

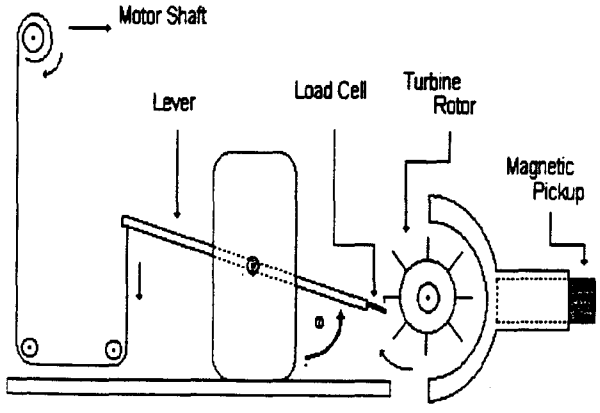

Figure 7 - Test rig for measuring the magnetic pickup

A turbine rotor prototype is placed under the effect of the magnetic field and in contact with the load cell. As the rotor has an even number of blades (eight) we used opposite blades to set up the test. The first blade is placed under the effect of the magnetic field and the fifth one is pressed by the load cell. The servo-motor moves the load cell upwards and against the magnetic force. The purpose of this movement is to take the system out of the equilibrium. The magnetic force is continuously recorded through the load cell, till the equilibrium is dismissed.

In order to simulate a real situation, the rotor was assembled keeping the same tip clearance and same distance between tip blades and the magnetic sensor. The rotor was free to turn restricted only by the bearing friction and the magnetic effect of the pickup. A punctual contact between the turbine blade and the load cell was adopted to reduce the influence of others frictions.

Figure 8, shows a record of the magnetic retarding force from the data acquisition system.

The x-coordinate of this figure shows the angle between the blade and the lever position.

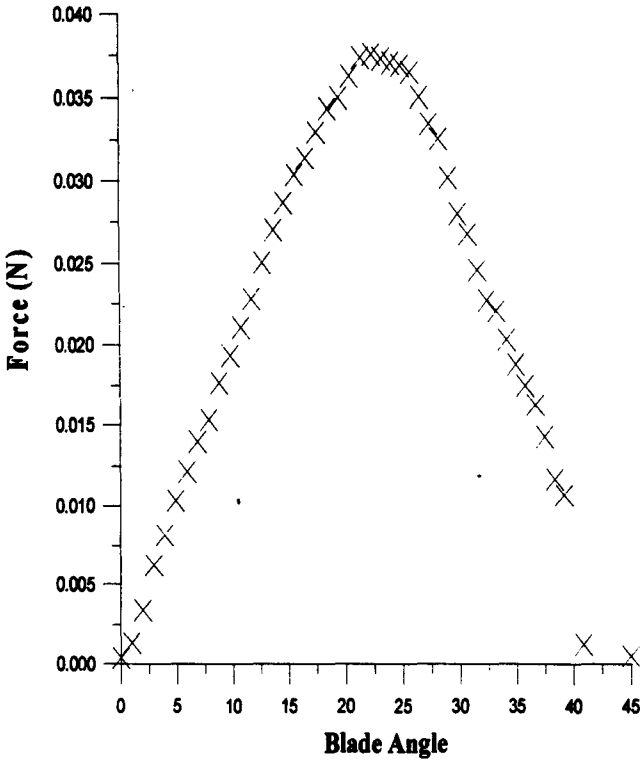

Figure 8 - Magnetic pickup retarding torque

From this figure (Fig. 8) one can easily see the distinct situations of the magnetic influence. The first region is the rising part of the curve, where the retarding force increases from zero up to the maximum value. The record reaches the maximum value when the contact between the cell and the blade is almost disconnecting. The following region shows the load cell relief during the rotor's turn. Figure 8 also shows a small step of discontinuity of the results happening about the blade angle of 40^0. This was due to vertical movement of the lever with the magnetic retarding effects acting one the approaching (the sixth) blade.

Actually, the data shown in Fig. 8 have an additional retarding effect. The bearing's static friction is always included in these records. In order to access the bearing static friction a set of measurement was taken with the same test rig. The same procedure was adopted, however, without the influence of the magnetic pickup. The magnetic pickup force is obtained by subtracting this value from the previous one (fig. 8). The bearing static friction measured was 0.003893 N $\pm$ 0.000641 N, so the maximum magnetic pickup retarding force was 0.03405 N $\pm$ 0.0016 N with an estimate uncertainty of $\pm$ 4.7% FS. The retarding torque can be calculated by multiplying the force value by the cantilever arm (30.9 mm) of the load cell.

The influence of the magnetic retarding torque on the turbine rotor is quite different from the previous retarding effects identified by the equilibrium equation (Eq. 1). This retarding effect oscillates from zero up to a maximum, every time a blade passes near by the pickup, whereas the other ones, act continuously depending, normally, on the rotational speed. The magnetic effects depend on the blade position, number **Z** of blades and on the rotational speed. It varies every angular sector of $2\pi/Z$ rad in a sinusoidal oscillatory feature as shown in figure 9. Figure 9 presents the variation of the magnetic pickup retarding torque for several rotational speed of the turbine flow meter prototype tested.

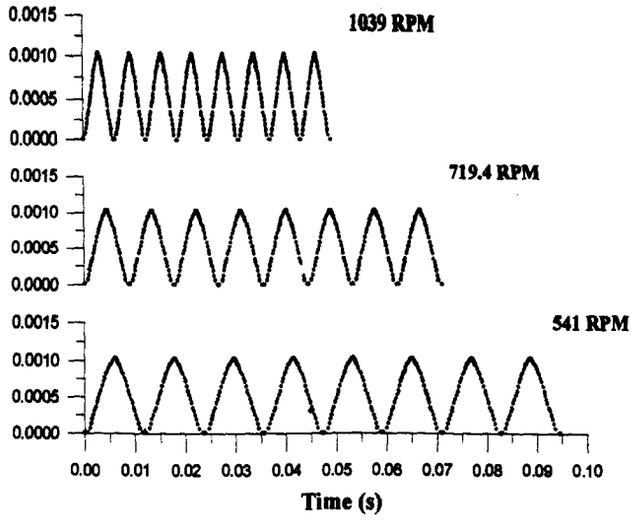

Figure 9 - Magnetic retarding torque versus rotatioanal speed

For the equilibrium equation (Eq. 1), though, the average value for a long period of time of the magnetic retarding effect is of interest. Thus, as the blade position is fixed with respect to the magnetic pickup, the average effect $\overline{T}_p$ can be calculated by the RMS of any result (curves) shown in figure 9 (T_{RMS}). The value of T_{RMS} remains constant (independent on the turbine rotational speed) and given, in Nm, as:

$$\overline{T}_p = T_{RMS} = 0.0003231743 \qquad (3)$$

The magnetic pick up also caused an electric generated power due to the running blades near by the magnetic field. The value of this effect was neglected due to the very low value obtained ($< 10^{-8}$ Nm).

THEORETICAL ANALYSIS

The left hand side of the equilibrium equation is identified as the *driving torque* and may be calculated using the angular momentum approach or by the airfoil theory.

The infinitesimal driving torque (dT_d), according to the angular momentum (Rubin et al., 1965), can be calculated as:

$$dT_d = 2\pi\rho V_Z^2 \left[\tan\beta_2 - \frac{\omega_a r}{V_Z}\right] r^2 \qquad (4)$$

where the variables V_z and β_2 are represented in figure 10, r is the radial coordinate, ω_a the rotational speed of the turbine meter and ρ the specific gravity.

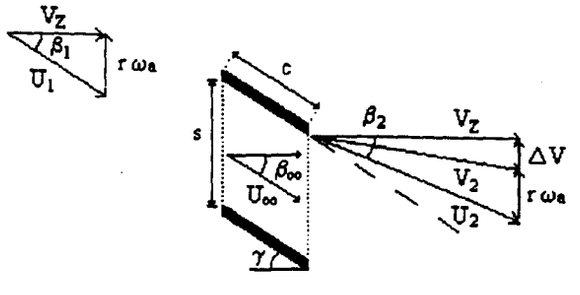

Figure 10 - Momentum approach for a constant blade angle γ

Applying the airfoil theory (Shepherd, 1969), the driving torque of any turbomachine may be obtained. If the blade surface drag is not the only retarding effect and is placed to the right hand side of the equation, the infinitesimal driving torque, for a turbine type flowmeter, will be given, by:

$$dT_d = \frac{1}{2}\rho V_Z^2 cZ\left[\frac{2\pi K_0 \sin\delta}{\cos\beta_\infty}\right] r\,dr \qquad (5)$$

where, K_0 is the cascade coefficient, c is the chord of the straight blade and δ ($\delta = \beta_1 - \gamma$) is the angle of incidence.

The outlet flow angle (β_2) differs from the blade angle (γ) due to the inability of the fluid to follow the blade. The actual value of β_2 is always difficult to be accessed. Theoretically, there are some approximate techniques to evaluate β_2. Experimentally, one may measure it by using Laser Doppler Velocimetry techniques (LDV). At the present work an analytical process described by Schlichting, 1959, was used. The experimental analysis with LDV is still under way.

Thus, for the previous equation (Eq. 5), β_∞ is calculated as:

$$\tan\beta_\infty = \frac{1}{2}(\tan\beta_1 + \tan\beta_2) \qquad (6)$$

where β_1 is the inlet flow angle. The difference between the blade angle γ and the inlet fluid angle β_1 is known as the angle of incidence δ. The blade angle of the present turbine prototype is $12{,}3^0 \pm 1^0$.

In order to integrate equations 4 or 5 all over the radial coordinate r one must know V_z (mean axial velocity) and the rotational speed ω_a. These two variables were obtained from the calibration curve of the turbine prototype so, for any particular flowrate one may obtain the V_z and ω_a.

The retarding torques, presented in the right hand side of Eq. 1, are calculated using the analytical expressions developed by Blows (1981), Rubin et. al. (1965), Thompson and Grey (1970) and Tsukamoto and Hutton (1985) or experimentally, already presented in this paper.

- The blade surface drag torque T_s, was expressed by:

$$T_s = \int dT_d = \frac{1}{2}\int \rho V_Z^2 cZ\left[\frac{C_D \sin\beta_\infty}{\cos^2\beta_\infty}\right] r\,dr \qquad (7)$$

where the C_D is the total drag coefficient of the blades. The total C_D included the blade surface drag, the induced drag (Senoo, 1987) and the wake effect due to the trailing edge (Klein, 1977).

The wake effect is function of the energy loss thickness δ_{3H}, at the trailing edge. This loss thickness was assumed to be of the order of three time the size of the blade thickness for both sides of the blade (suction and pressure side). This assumption is supported due to the straight blade shape adopted in this turbine flow meter. This straight blade prototype has no cusp at the trailing edge.

- The rotor hub friction torque T_h, is expressed using the following expression presented by Thompson (1970):

$$T_h = \frac{1}{2} Z \rho V_z^2 C_D CS \cos\gamma \left[\left(\frac{q}{1+q} \right) \tan\gamma + \left(\frac{1}{1+q} \right) \tan\beta_1 \right] \left\{ 1 + \left[\left(\frac{q}{1+q} \right) \tan\gamma + \left(\frac{1}{1+q} \right) \tan\beta_1 \right]^2 \right\}^{\frac{1}{2}} r_h \quad (8)$$

where q is function of the space-to-chord ratio (s/c) and defined as:

$$q = \frac{\pi K_0}{2s/c} \cos\gamma \quad (9)$$

Another expression for the T_h was used based on the skin friction for rough surface presented by Schlichting, 1960. The results obtained showed not much difference from the previous expression (Eq. 8).

- The disk surface slip drag between the rotor hub and the support T_f, is expressed by Eq. 10 (Favaretto, 1995):

$$T_f = \frac{2}{\Delta z} \pi \omega_a \mu \left(r_c^2 - r_e^2 \right) \left(r_c - r_e \right) \left[r_e + 2/3 \left(r_c - r_e \right) \right] \quad (10)$$

where μ is the absolute viscosity, r_c and r_e the radial coordinate of the hub and the shaft of the prototype rotor, respectively. Δz is gap between rotor hub and support.

- The retarding torque due to the blade tip clearance, T_{bt}, is given by Eq. 11 (Thompson, 1970):

$$T_{bt} = \frac{0{,}078}{2\,\mathrm{Re}^{0{,}43}} \rho\, \omega_a^{\,2}\, r_t^{\,3}\, c\, t\, Z \quad (11)$$

where R_e is Reynolds number, r_t radial coordinate of the blade tip and t the thickness of the blade. The Reynolds number is function of the tip clearance Δr and defined as:

$$R_e = (\rho/\mu)\, \omega_a r_t\, \Delta r \quad (12)$$

Another expression may be used to evaluate the blade tip clearance torque, based on the journal bearing analogy proposed by some authors. The following expression (presented by Blows, 1981) was also tested with similar results of Eq. 11:

$$T_{bt} = 4\pi^2 \omega_a \mu c r_p^{\,3} \cos\gamma / (r_p - r_t)^3 \; F_A \quad (13)$$

where r_p is the radius of the turbine meter case and F_A is the area factor, that is, a percentage of the tip area to the total case area.

- The bearing retarding torque T_{brl}, measured experimentally, was expressed by previous equation (Eq. 2).

- The mean magnetic pickup torque $T_p = \overline{T}_p$, is constant (that is independent on the rotational speed), and is given by the Eq. 3.

With the above expressions it is possible to calculate the right hand side of Eq. 1. Figure 11 shows a comparison between the driving torque, left hand side of Eq.1, and the summation of the retarding torques. As one can see from this figure the maximum difference between the driving and retarding torque is about 10%. This difference, which is due to the analytical models adopted for the driving and retarding torques, remains as a challenge for improving this work in the near future.

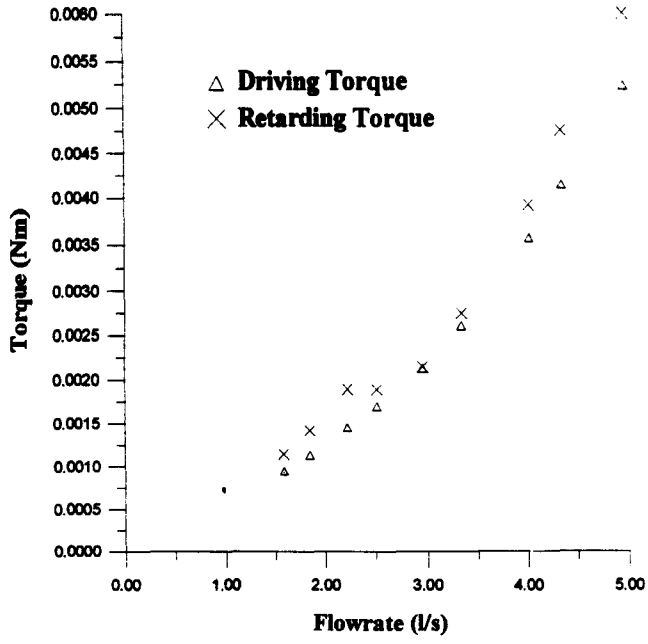

Figure 11 - Comparison between driving torque and retarding torques

PERFORMANCE ANALYSIS

The influence of the magnetic pickup on turbine meter performance was also analysed based on the calibration curves. The two different situations were studied: with and without the influence of the magnetic pickup. The calibration curves were obtained using the water test facility described by Ferreira et al. (1991). The test rig is an intermittent gravimetric calibration system for water flowmeters ranging from 0.1 up to 5 *l*/s with an uncertainty ±0.5% FS. The following figure (Fig. 12) presents the two calibration curves. In this figure, **Ki** (%) represents a percentage deviation coefficient from the meter factor $\overline{K}$ (litres/pulse), as a function of the flow rate.

To eliminate the magnetic effect an optical pickup was developed using an infrared emitter/receptor device. The new pickup produced no detected retarding effect on the meter rotor.

From figure 12 it is apparent that the friction produced by the magnetic effect is important at the beginning of the calibration curve. The magnetic pickup caused a significant delay in the motion of the turbine meter. Therefore, without magnetic retarding torque, the turbine started running at much lower flow rate (0.73 *l*/s) than with the magnetic sensor (1.067 *l*/s). Thus, using an optical pickup, the "operational range" of this prototype increased from about 28%.

Assuming that the "usage flow range" of the prototype tested is the region of the calibration curve where the meter factor (K) lays within the linearity of ±2.5%, is easy to see, from figure 12, that the useful flow range is smaller for the magnetic pickup than for the optical one.

The linearity of the calibration curve, apart from the beginning part, did not show significant changes. Although the flow range tested not included the whole range it is believed that the behaviour of the calibration curve would not be affected a high flow ranges. As was shown previously, the magnetic retarding torque is constant (independent on the rotational speed) and

ESCOLA DE ENGENHARIA

the remaining retarding torques depend upon the rotational speed (N) or/and on the flow rate. Therefore, the greater is the flow rate the least significant is the magnetic effect.

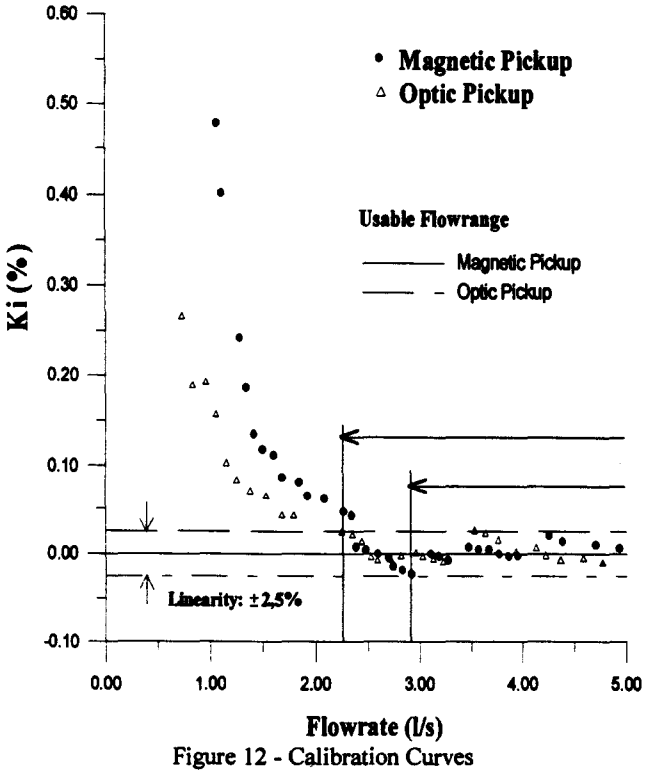

Figure 12 - Calibration Curves

CONCLUSION

The equilibrium equation presented by this analytical/ experimental model showed reasonable good results comparing the right with the left hand side. A comparison for the driving torque of both theories, airfoil and momentum, presented some disagreements along the whole range tested. There are some reasons for this divergence: a) to assume V_z constant, instead of an inlet velocity profile and b) to calculate the outlet flow angle β_2, instead of measuring experimentally. These are the most important reasons, according to the authors.

The use of the magnetic pickup signal alters the turbine meter performance only in the beginning region of the calibration curve. This is important because affects the operational range and also the useful flow range. The substitution of the magnetic pickup for an optical or an RF pickup type will increase the flow range allowing measurements at much lower flow rates.

The perfect knowledge of the retarding effects of a turbine flow meter will allow to predict the performance and to improve the design of new prototypes.

ACKNOWLEDGEMENTS

The authors would like to thank the Turbomachinery and Flow Measurement Laboratory staff for the contributions received and CNPq for the financial support received in this project.

REFERENCES

Blows, L.G., 1981, "Towards a better Turbine Flowmeter- International Conference on Advances in Flow Measurements Techniques" - paper L3, University of Warwick, UK, England.

Favaretto, C. F. F., 1995, "Medição do Torque Resistivo em Turbinas de Medição", Internal Report, CNPq. LTMF - UFRGS, Porto Alegre.

Ferreira, V. C. S., Souto, S.L.L. and Schuller, M.B., 1991, "Medidores de Fluxo: Obtenção da Curva de Calibração via Terminal Inteligente", XI COBEM, Proceedings, pp 49-52, S.Paulo.

Ferreira, V. C. S., 1994, "Estudo Experimental do Atrito Mecânico em Turbinas de Medição", 10º Seminário de Instrumentação do IBP, Proceedings, pp 216-225, Porto Alegre.

Klein, A., 1977, "Aerodynamics of Cascades". AGARD-AG-220, NATO, Verlag G. Braun.

Rubin, M., Miller, R.W. and Fox, R.W., 1965, "Driving Torques in Theoretical Model of a Turbine Meter"- Journal of Basic Eng. Trans. ASME. pp 413-420.

Schlichting, H., 1959, "Application of the boundary layer theory in turbomachinery", Trans. ASME, J. of Basic Engineering, 81, pp 543-551, NY.

Schlichting, H., 1960, "Boundary Layer Theory", 4th ed. McGraw-Hill, Ney York.

Senoo, Y, 1987, "Pressure Losses and Flow Field distortion Induced by tip Clearance of Centrifugal and axial Compressors". JSME, Int. Journal, Vol 30, No. 261, pp375-385.

Shepherd, D.G., 1969, "Principles of Turbomachinery", 9th Ed. The Macmillan Company, Collier-Macmillan Canada, Ltd. Toronto, Ontario.

Thompson, R.E. and Grey, J., 1970, "Turbine Flowmeter Performance Model"- Journal of Basic Eng., Trans. ASME, pp 713-722.

Tsukamoto, H. and Hutton, S.P., 1985, "Theoretical Prediction of Meter Factor for a Helical Turbine Flowmeter", Fluid Control and Measurements - Meiji University, Tokyo.

Ferreira, V.C.S. and Venzon, M.C. P., 1995, "Orifice Plate Behavior in Two Phase Flow (Air-Water)". COBEM-CIDIM/95, UFMG, Proceedings (Compact Disk), Belo Horizonte.